International Journal of Cancer / Volume 130, Issue 9

Cancer Therapy | Free Access

ROS implication in a new antitumor strategy based on non-thermal plasma

Marc Vandamme, Eric Robert, Stéphanie Lerondel, Vanessa Sarron, Delphine Ries, Sébastien Dozias, Julien Sobilo, David Gosset, Claudine Kieda, Brigitte Legrain, Jean-Michel Pouvesle, Alain Le Pape

First published: 23 June 2011
https://doi.org/10.1002/ijc.26252
Cited by: 234

Abstract

Non-thermal plasma (NTP) is generated by ionizing neutral gas molecules/atoms leading to a highly reactive gas at ambient temperature containing excited molecules, reactive species and generating transient electric fields. Given its potential to interact with tissue or cells without a significant temperature increase, NTP appears as a promising approach for the treatment of various diseases including cancer. The aim of our study was to evaluate the interest of NTP both *in vitro* and *in vivo.* To this end, we evaluated the antitumor activity of NTP *in vitro* on two human cancer cell lines (glioblastoma U87MG and colorectal carcinoma HCT-116). Our data showed that NTP generated a large amount of reactive oxygen species (ROS), leading to the formation of DNA damages. This resulted in a multiphase cell cycle arrest and a subsequent apoptosis induction. In addition, *in vivo* experiments on U87MG bearing mice showed that NTP induced a reduction of bioluminescence and tumor volume as compared to nontreated mice. An induction of apoptosis was also observed together with an accumulation of cells in S phase of the cell cycle suggesting an arrest of tumor proliferation. In conclusion, we demonstrated here that the potential of NTP to generate ROS renders this strategy particularly promising in the context of tumor treatment.

in industry[1] and in medicine.[2, 3] Recently, the development of a new kind of plasma devices generating non-thermal plasma (NTP) has extended their potential applications especially in biology and medicine.[4-6] NTP with a temperature less than 40°C at the point of treatment is a partially ionized media generated by excitation of a gas mixture in a discharge reactor. It contains electrons, positive/negative ions, radicals, various excited molecules, energetic photons (UV) and generates transient electric field. Given these interesting properties, potential

The dose of NTP delivered is an important parameter to induce biological responses in tissue and cells.8 Indeed, low dose of plasma (<1 J cm^{-2}) is able to induce inactivation of bacteria and proliferation of cells,11, 12 while higher dose (>7 J cm^{-2}) can induce apoptosis of tumor cells including melanoma, breast cancer cells and hepatocellular carcinoma.13-17 Sensenig *et al.* and Kim *et al.* have suggested that DNA damages and reactive species generated by plasma could be the main causes of this effect.14, 18 In a recent work, Kalghatgi *et al.* showed that a low dose of NTP enhances endothelial cell proliferation due to the reactive oxygen species (ROS) generated by NTP mediated FGF-2 release.11 On non-tumorigenic breast epithelial cell line, NTP was also recently described to induce DNA damage leading to apoptosis due to the formation of intracellular ROS.19 ROS are potentially harmful on cellular metabolism by affecting cell functions with a direct effect on cell development, growth, survival as well as tumorigenesis.20 As described for NTP, the effect of ROS on cells is dose-dependent. While low doses of ROS induce mutagenesis and cell proliferation, high levels not only inhibit cell proliferation, but also induce a high cytotoxic effect to the cell and can lead to apoptosis of a wide range of tumors.20-22

Radiotherapy mechanisms are also based on the formation in targeted cells of ROS including superoxide, hydrogen peroxide and free hydroxyl, that are able to induce lethal DNA damages which activate cell cycle checkpoints and initiate signaling cascades leading to cell death.23, 24 NTP, thanks to its ability to generate *in situ* ROS at the vicinity of the tumor, appears thus as a good candidate for cancer treatment. Indeed, recent development in plasma sources allows the propagation of cold plasma in small capillary as plasma jet,25 so opening perspective to treat such tumor types as colorectal, lung or pancreas tumor with a flexible micro plasma endoscope (Fig. 1). A preliminary survival study has shown an antitumor activity of plasma floating electrode dielectric barrier discharge (FE-DBD) *in vivo* with a significant lifespan increase in mice bearing U87MG malignant glioma.26 This plasma is generated in the gap between an insulated high voltage electrode and the skin or the tissue (floating electrode) (Fig. 1). Very few studies have described mechanisms implied in the effect of NTP on tumor cells and further characterization of global effect of plasma on cells is needed.

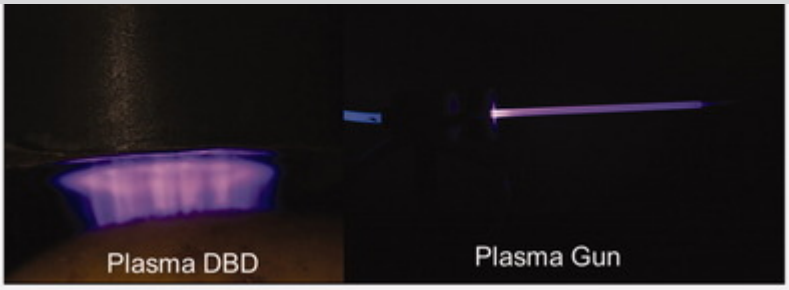

Non-thermal plasmas. NTP generated with DBD system (left panel). NTP generated at the extremity of a very small capillary so called “plasma gun” (right panel), plasma expands over 12 cm in a 4 mm inner diameter glass capillary and then in ambient air along about 2 cm.

Caption

The aim of this work was to evaluate antitumor effect of NTP *in vitro* along with mechanisms underlying massive cell death induction. We first documented the in *vitro* antitumor activity of plasma using MTT and bioluminescence assay. Then, we considered the role of ROS in this antitumor activity as well as formation of DNA strand breaks, cell cycle modifications and apoptosis induction.

On U87MG glioma bearing mice, we evaluated effect of NTP on tumor volume and the consequences of treatment on cell proliferation, cell cycle and apoptosis induction. For such a goal, bioluminescence imaging (BLI), an imaging modality dependent on cell metabolism and proliferation, is a unique resource when exploited in association with cellular biomarkers.

Abbreviations

BLI: bioluminescence imaging; BrdU: bromodeoxyuridine; DHE: dihydroethidium; DNA: deoxyribonucleic acid; FE-DBD: floating electrode dielectric barrier discharge; FITC: fluorescein isothiocyanate; FLI: fluorescence imaging; H2DCFDA: 2, 7-dichlorodihydrofluorescein diacetate; MTT: 3-(4,5-dimethylthiazol-2-yl)-2,5-diphenyltetrazolium bromide; NAC: *N*-Acetyl-L-cysteine; NTP: non-thermal plasma; ROS: reactive oxygen species; RS: reactive species

Material and Methods

Cell culture

U87MG-Luc2 and HCT-116-Luc2 Bioware Ultra cell lines were purchased from Caliper® (Caliper Life Sciences, Roissy, France) and maintained in a humidified incubator containing 5% CO_2 at

and 1% penicillin-streptomycin (10,000 U/mL). Both cell lines are stably transfected with firefly luciferase gene, thus allowing BLI.

Animals and tumors

Swiss nude female mice, 4 weeks of age, were purchased from Charles River® (Saint-Germain-sur-l'Arbresle, France) and acclimated for 1 week in the laboratory before experimentation. Animals were housed in plastic cages inside a controlled ventilated rack with free access to

(Aerrane®, Maurepas, France). Tumor xenografts were achieved by subcutaneous injection of tumor cells suspension (10^6 cells in 0.1 mL 0.9% NaCl) into the hind legs. To follow tumor growth, tumor volume (V in mm^3) was measured with a caliper and was calculated as $V = (\text{length} \times \text{width}^2)/2$.

Plasma treatment

Plasma was generated with a FE-DBD by applying a microsecond pulse voltage of 23 kV. Plasma is generated in open air in the gap fixed at 2 mm between the insulated electrode (one mm thick glass) and the sample. Discharge power density of our DBD was 0.52 watts at 2000 Hz, thus a 15s treatment using the 0.78 cm^2 insulated reactor lead to a dose of 10 J/cm^2. More detailed characteristics of plasma sources are presented in Supporting Information.

In *in vitro* experiments, U87MG and HCT-116 cells ($1x10^5$) were seeded in 24-well plates 24 hr before plasma treatment. Direct plasma treatment of cells seeded in 24-well plates was performed in open air, 2 mm upper the medium of each well containing adherent cells and 500 µL of medium (Supporting Information Fig. S1). For indirect treatment, plasma was applied in a well containing 500 µL medium only (without cells). Then, treated medium was immediately and carefully dropped in wells containing cells. During these two exposure conditions, the increase in temperature of the medium was observed to be less than 1°C and no significant pH modification was observed (data not shown).

For *in vivo* studies, when tumors reached a volume of 125 ± 50 mm^3 (D0), mice were randomly assigned into two groups. In the CTRL group, mice were not treated while in NTP group, mice received plasma treatment. Each group of treatment included 16 mice. Tumor treatment was performed daily at 200 Hz during 6 min for five consecutive days (corresponding to 120 J/cm^2/day), this treatment dose was previously determined with a tolerance study.[26] During all treatment procedure anesthetized mice were placed on a temperature regulated silver plate and plasma reactor was positioned at a distance of two millimeters above the tumor (Supporting Information Fig. S1). After 24 hr of the last day treatment, all tumors were excised

Bioluminescence

Tumor growth of treated and nontreated mice was monitored by tumor volume measurement and BLI. BLI is an imaging modality allowing the evaluation of very early stages of antitumor effect prior to physical reduction of the tumor and bioluminescence intensity is closely dependent on the tumor activity.

were intraperitoneally injected with 100 mg/kg luciferin potassium salt (Promega, Paris, France) and imaging was acquired 6 min after substrate injection under general anesthesia in the dark box of a high sensitivity CCD camera cooled to −90°C (IVIS Lumina II, Caliper Life Sciences, Roissy, France). Acquisition settings (binning and duration) were set up depending upon tumor activity at the time of the acquisition and images were acquired and analyzed using Living Image software (Caliper Life Sciences, Roissy, France).

Cell growth assay

HCT-116 and U87 cell number and cell growth inhibition by NTP were determined by trypan blue exclusion assay, by BLI and by measuring 3-(4,5-dimethylthiazol-2-yl)-2,5-diphenyltetrazolium bromide (MTT) dye absorbance by living cells. Cells were treated as described and incubated for additional 24 hr. *In vitro* BLI: 300 µg/mL luciferin potassium salt (Promega, Paris, France) was added in the well plate and the BLI was recorded after 5 min incubation at 37°C using IVIS Lumina (Caliper). BLI intensity of each well in photon/sec was normalized to nontreated cells. Concerning MTT assay, MTT solution (2.5 mg/mL in PBS) was added to each well and cells were incubated for 4 hr. Formazan crystals resulting from MTT reduction were dissolved by the addition of 10% SDS in DMSO/acetic acid solution per well. The relative quantity of formazan products formed in each well was detected by reading absorbance at 570 nm.

ROS inhibition

To inhibit ROS, *N*-acetyl-L-cysteine (NAC, Sigma-Aldrich, Lyon, France), an intracellular ROS scavenger, was used. Cells were pretreated with 4 mM NAC for 30 min prior treatment by NTP.

Detection of ROS levels in the medium

ROS such as H_2O_2, $^{\bullet}OH$ and $ONOO^{\bullet}$ were detected using an oxidation-sensitive fluorescent probe dye 2, 7-dichlorodihydrofluorescein diacetate (H_2DCFDA, Sigma-Aldrich, Lyon, France, Ex/Em = 495/529 nm). As H_2DCFDA is poorly selective for $O_2^{\bullet-}$, dihydroethidium (DHE, Sigma-

detection (detailed in Supporting Information). Fluorescence was acquired using IVIS Lumina with the suitable filters and analyzed with Living Image software (Caliper Life Sciences, Roissy, France).

Apoptosis detection

In vitro, cell apoptosis was measured 24 hr after NTP by flow cytometry using an annexin V-FITC apoptosis detection kit (R&D Systems, Lille, France). Non adherent and adherent cells were

cytometry using a FACSort (Becton and Dickinson, Le pont de Claix, France).

In vivo, 24 hr after the end of the treatment, tumors were excised and apoptosis indexes were determined by immunohistochemistry detection of cleaved caspase 3 with SignalStain Cleaved Caspase-3 IHC kit (Cell Signaling, Saint Quentin Yvelines, France) according to the manufacturer. These experiments were realized under double blind analysis in collaboration with Novaxia, Saint Laurent Nouan, France, a company specialized in histology-pathology. The percentage of labeled tumor cells was evaluated in adjacent areas of the tumor mass free from necrosis. Additional details are given in Supporting Information.

Cell cycle analysis and cell proliferation

Cell cycle analysis was performed 24 hr after NTP by combined propidium iodide and bromodeoxyuridine (BrdU, Sigma-Aldrich, Lyon, France). Briefly, after methanol fixation and Triton X-100 permeabilization, cells were incubated for 30 min with fluorescein isothiocyanate (FITC)-conjugated anti-BrdU antibody (7 µg/mL, Millipore, Molsheim, France). An IgG1 mouse secondary FITC-conjugated (Millipore, Molsheim, France) was used as negative control for non-specific fluorescence. As a positive control, we used cells treated by topotecan (0.2µM). Cells were finally incubated with 5 µg/mL propidium iodide (Sigma-Aldrich, Lyon, France) prior to analysis using a FACSort (Becton and Dickinson, Le pont de Claix, France). Additional details are given in Supporting Information.

Cell cycle distribution *in vivo* was determined by DNA content analysis after propidium iodide staining as described earlier.27, 28 Briefly, tumor samples were incubated with trypsin (0.03 mg/mL) and were dissociated using a Potter pestle. Samples were then treated with RNAse A (0.1 mg/mL) and incubated with propidium iodide (0.4 mg/mL) for 30 min in the dark. Then samples were filtered on a nylon mesh prior to analysis using a FACSort (Becton and Dickinson, Le pont de Claix, France).

DNA damages

by flow cytometry was performed 1 hr after treatment using γH2AX phosphorylation Assay Kit (Millipore, Molsheim, France) in accordance with manufacturer protocol. Briefly, after ethanol fixation and saponin cell permeabilization, histone H2AX phosphorylated at serine 139 was detected by the addition of the antiphospho-Histone γH2AX, FITC conjugate. As a negative control for nonspecific binding an IgG1 mouse secondary FITC-conjugated (Millipore, Molsheim, France) was used. As a positive control, we used cells treated by topotecan (0.2µM). The degree

Statistical analysis

Unless otherwise noted, data were reported as a mean ± SEM. Mann-Whitney test was used to evaluate the statistical significance of the results. DL50 were determined according to the Hill slope method (GraphPad Prism 5.0, La Jolla, CA, USA). Differences were considered significant at p values < 0.05. For all cytometry analyses, RAW data are presented in Supporting Information Figure S2.

Results

NTP presents a major antitumor effect *in vitro*

We first evaluated the antitumor potential of NTP on two different cell lines *in vitro* using cell viability (cell counts) and metabolism assays (MTT and BLI). As described in Table 1, 24 hr after treatment, NTP induced a major decrease in cell number as compared to CTRL. In U87MG cell line, a 10 J/cm^2 treatment induced a 46% significant decrease in living cells (p = 0.04) associated to 312% significant increase in dead cells (p = 0.02). Using 20 J/cm^2, almost all cells were dead after 24 hr. These results are in accordance with metabolism assays, which showed a similar decrease in cell viability for the two cell lines with both MTT and BLI (Figs. 2*a*, 2*b* and Supporting Information Fig. S3). The DL_{50} was ~9 J/cm^2 in U87MG and ~8 J/cm^2 in HCT-116, respectively. To understand which components of plasma are involved in this effect, further investigations were realized using both MTT and BLI. Considering the concordance between these two tests, only BLI data are presented.

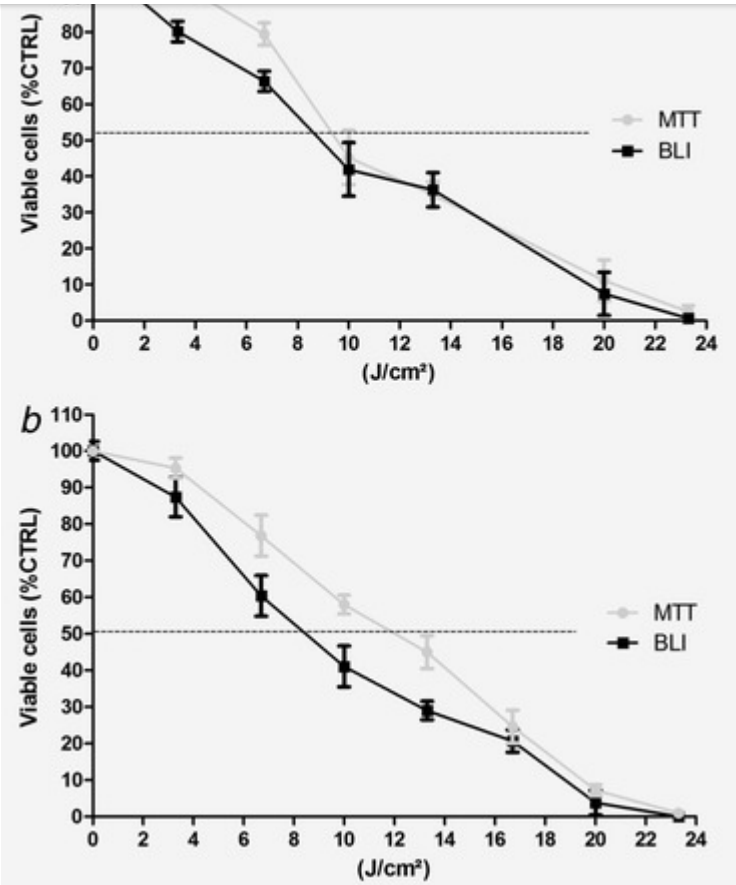

Figure 2

Open in figure viewer | PowerPoint

Antitumor responses to NTP treatments. U87MG (*a*) and HCT-116 (*b*) cells were treated by increasing doses of NTP. Cell viability was determined 24 hr after treatment by both MTT (•) and BLI (▪) assays. Cell viability of NTP treated cells was normalized to untreated cells.

Caption

	U87		HCT-116	
Groups	Living cells	Dead cells	Living cells	Dead cells

Data are presented as mean ± SEM.
*$p < 0.05$; **$p < 0.01$ *vs.* CTRL.

Plasma generated species in the culture medium are the main cause of cell death

To identify plasma components implicated in cell death, direct and indirect treatments were performed. For U87MG, 10 and 20 J/cm^2 direct plasma treatment induced a 40% and 96% decrease in cell viability, respectively (p = 0.009 and p = 0.01). As shown in Figure 3*a*, a similar decrease was observed for both direct and indirect treatment. The same results were observed using HCT-116 cells (Supporting Information Fig. S4a). To confirm the implication of the NTP treated culture medium in this effect, a quantification of ROS production was performed with an oxidation-sensitive fluorescent probe dye. In Figure 3*d*, using H_2O_2 specific dye (H_2DCFA), 10 or 20 J/cm^2 NTP induced a 5 fold and a 7 fold increase in levels in the medium, respectively (p = 0.002 and p = 0.002). Normalization with H_2O_2 standard concentrations revealed that plasma generated an equivalent concentration of 600 µM H_2O_2 for 10 J/cm^2 and 900 µM H_2O_2 for 20 J/cm^2 treatments.

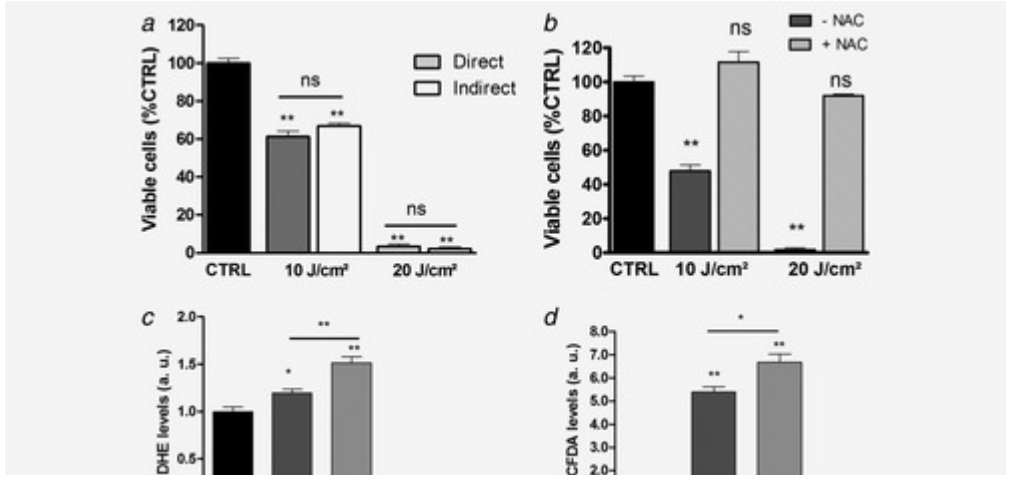

Figure 3

ROS implication in the antitumor effect of NTP. (*a*) A direct and indirect treatment was performed on U87MG and cell viability was determined by BLI imaging and was normalized to non-treated cells (CTRL). (*b*) U87MG cells were pretreated with NAC (4

(H_2DCFDA), fluorescence levels were expressed as normalized fluorescence intensity. (*d*) A second dye Dihydroethidium (DHE), which is highly selective for $O_2^{\bullet-}$ was used, fluorescence levels were expressed as normalized fluorescence intensity. *$p < 0.05$; **$p < 0.01$.

Caption

A second dye with a high specificity for O_2^- (DHE) showed an increase in ROS in the both group of treatment (Fig. 3*c*); 20% for 10 J/cm^2 ($p = 0.02$) and 52% for 20 J/cm^2 ($p = 0.002$). To confirm the implication of ROS, cells were pre incubated with intracellular ROS scavenger NAC, followed by NTP treatment (Fig. 3*b*). After 24 hr, CTRL cells and CTRL cells with NAC alone did not evidence any cell viability modification (data not shown). In NAC pretreated groups, no significant decrease in cell viability was observed for both NTP doses, as compared to CTRL. Similar results were observed in HCT-116 cell line (Supporting Information Fig. S4b).

NTP induces a cell cycle arrest and an apoptosis induction

To determine the effect of plasma on cell cycle distribution, an iodide propidium staining was performed 24 hr after plasma treatment. In U87MG cells, plasma induced a significant decrease of cells in G0/G1 phase with a significant increase in cells in S-phase for 10 and 20 J/cm^2 groups as compared to CTRL (Fig. 4*a*). Concerning G2/M phase, a significant increase was observed only with 10 J/cm^2 of plasma ($p = 0.005$).

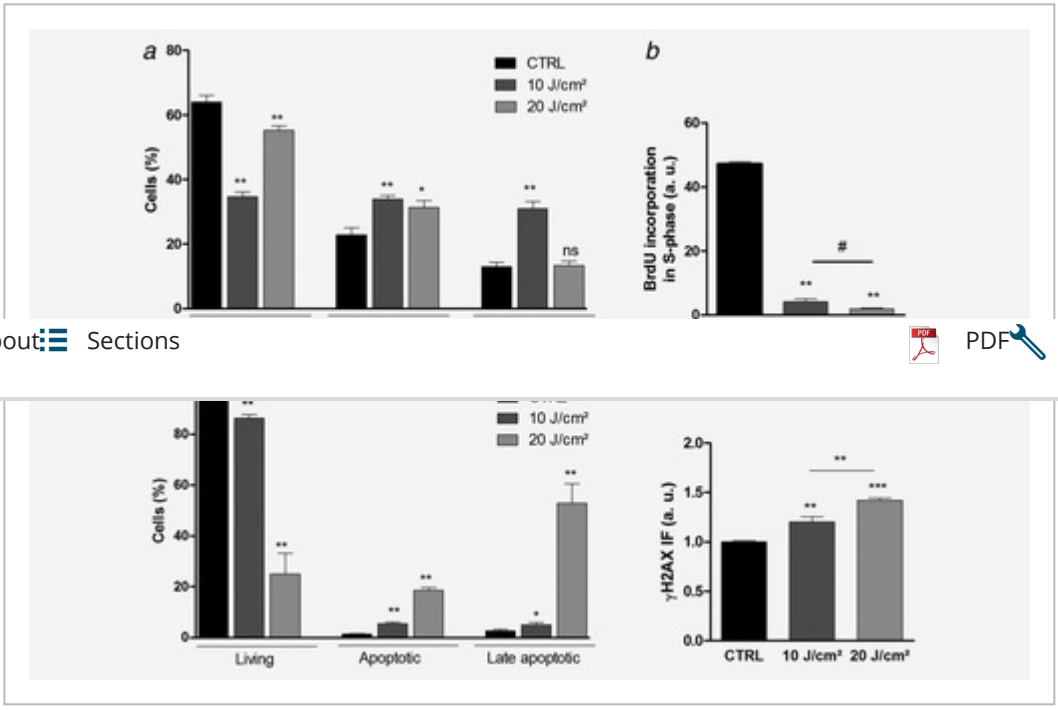

Cellular effects of NTP on U87MG cells. U87MG cells were NTP treated using two different doses (10 J/cm^2 and 20 J/cm^2). (*a*) Cell cycle distribution: 24 hr after treatment, cell cycle distribution was assessed by flow cytometry after propidium iodide staining. (*b*) Cell proliferation was evaluated by incorporation of BrdU into S phase by flow cytometry. (*c*) Cell apoptosis was measured 24 hr after NTP treatment by annexin V-propidium iodide labeling. (*d*) DNA damages induction: assessment of γH2AX immunofluorescence (IF) by flow cytometry was performed 1 hr after treatment. γH2AX IF was normalized to nontreated cells. *$p < 0.05$; **$p < 0.01$; ***$p < 0.001$.

Caption

In HCT-116 cells, plasma induced also a significant decrease in G0/G1 cells for both doses ($p = 0.002$) while a significant increase in cells in S phase was observed for 20 J/cm^2 only ($p = 0.002$; Supporting Information Fig. S5a).

A significant increase in cells in G2/M phase was observed for both treated groups as compared to CTRL ($p = 0.005$). These results suggested an accumulation of cells resulting from a cell cycle arrest, so a cell proliferation assay with BrdU incorporation was performed.

In U87MG (Fig. 4*b*), NTP induced a 92% and 97% decrease in BrdU incorporation for 10 and 20 J/cm^2, respectively ($p = 0.005$). Similar results were observed in HCT-116 cell line (Supporting Information Fig. S5b).

To determine whether the decrease in cell proliferation and the cell cycle arrest lead to apoptosis induction, an annexin V staining was performed 24 hr after the treatment. As presented in Figure 4*c*, plasma treatment induced apoptosis induction in both cell lines. In U87MG cells, both doses resulted in 3 and 12 fold increase as compared to CTRL group, respectively ($p = 0.002$). In HCT-116, this apoptosis induction was observed for both treated groups (Supporting Information Fig. S6a). For both cell lines, a significant increase in late apoptosis (Annexin V$^+$/PI$^+$) was also observed. Moreover, the presence of cells in late apoptosis was further confirmed by the observed induction of capase3/caspase 7 activity 24 hr after plasma application (Supporting Information Fig. S7).

NTP induces DNA damages

To determine whether plasma treatment induced DNA damages, assessment of γH2AX IF by flow cytometry was performed 1 hr after treatment. In both cell lines, a major increase in γH2AX IF was observed after 10 or 20 J/cm^2 of NTP. For U87MG (Fig. 4*d*), NTP induced a significant increase of 20 and 40% of γH2AX IF in 10 or 20 J/cm^2 group, respectively ($p = 0.002$; *p*

NTP exhibits a significant antitumor effect *in vivo*

Plasma was applied each day during 5 consecutive days on subcutaneously U87MG-Luc grafted tumors. Tumors were included in treatment groups when they reached 125 ± 50 mm^3. Mean tumor volumes were similar between the two groups: at D0, mean tumor volumes ± standard error in CTRL and treated mice were 129 ± 13 mm^3 and 124 ± 14 mm^3, respectively. To determined effect of NTP on tumor cell proliferation and metabolism, BLI was performed before (D0), during (D3) and after (D5) treatment course (Figs. 5*a* and 5*b*). In non-treated and treated mice groups, BLI activity showed 3 fold increase between D0 and D3 ($p < 0.0001$). From D3 to D5 a twofold increase was observed for the CTRL group only ($p = 0.02$), while in plasma treated tumors, BLI intensity remained stable over the D3-D5 period.

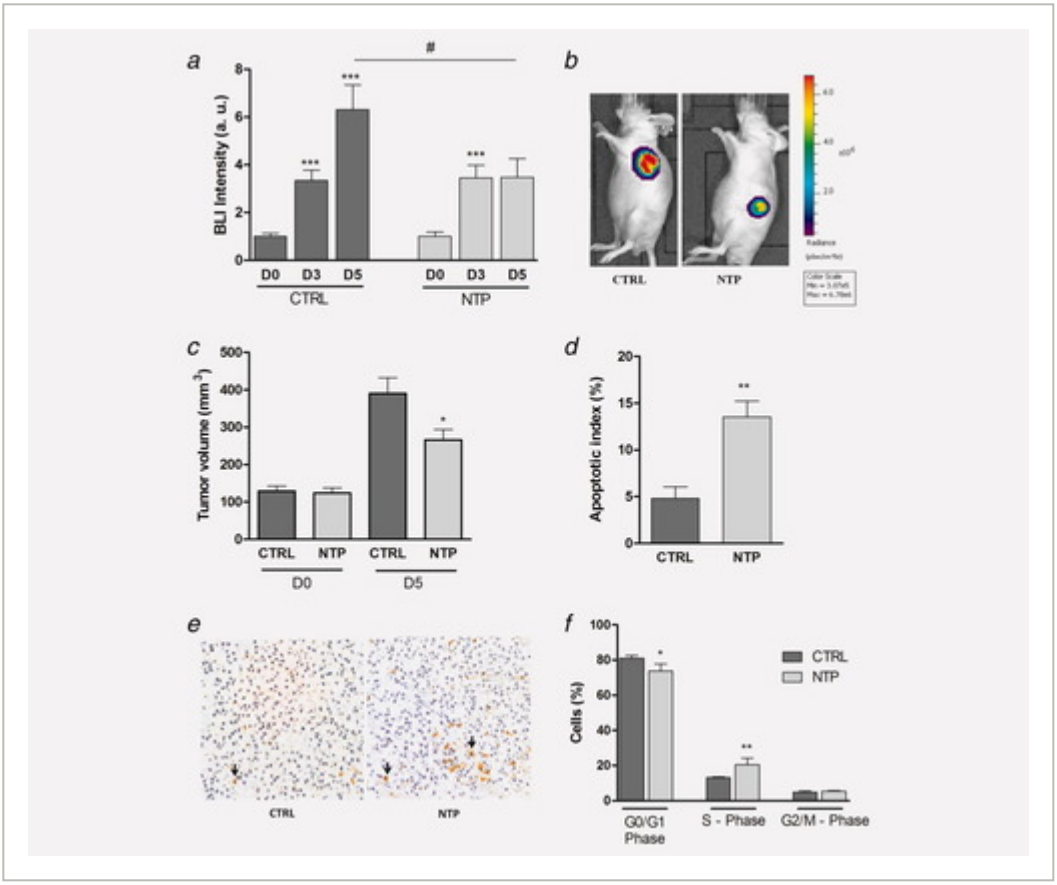

Figure 5

Open in figure viewer | PowerPoint

In vivo evaluation of NTP antitumor activity. When tumor reached 150 ± 50 mm^3, mice were randomly assigned into two groups: control (CTRL) and plasma, eight mice per group. Plasma treatment was delivered each day for five consecutive days (6 min, 200 Hz). Mice in both groups were sacrificed 24 hr after the last treatment. (*a*) BLI imaging was performed before the first treatment (D0), during treatment

of treatment (D5). (*d*) Apoptosis indexes were determined by immunohistochemical detection of cleaved caspase 3. (*e*) Representative cleaved caspase 3 immunostaining obtained in CTRL and NTP-treated tumors. Magnification x400. (*f*) Cell cycle distribution was assessed by flow cytometry after propidium iodide staining. *,# $p < 0.05$; *** $p < 0.001$.

Caption

Tumor volume measurements performed 24 hr after the end of the treatment course (Fig. 5*c*) revealed a significant lower tumor volume in the treated group (233 mm^3) as compared to CTRL (400 mm^3), ($p = 0.008$).

NTP induces a cell cycle arrest and apoptosis in tumor

To determine whether plasma induced apoptosis in these tumors, a caspase 3 immunostaining was performed 24 hr after the last day of treatment (Figs. 5*d* and 5*e*) resulting in a significant 3 fold increase in caspase-3 positive cells ($p = 0.008$). Positive cells for caspase 3 immunostaining represented 4.5 and 13.5% of tumor cells for CTRL and treated tumors, respectively. Moreover, caspase 3 positive cells were homogeneously distributed in sagittal sections from treated tumors.

Consequences of plasma on cell cycle distribution were determined 24 hr after the last day of treatment (Fig. 5*f*). As observed *in vitro*, propidium iodide staining showed a significant decrease in G0/G1 cells in tumor after treatment as compared to CTRL ($p = 0.022$). Cells in G0/G1 phase decrease from 81% to 73% after NTP and this effect was associated with a significant 1.5 fold increase in cells in S phase ($p = 0.002$) from 13 to 20% in CTRL and Plasma groups, respectively.

Discussion

In this study, we evaluated the antitumor potential of NTP on two different cell lines and determined some of the underlying biological mechanisms. Metabolism assays showed that NTP had a significant antitumor activity on U87MG and HCT-116 cell lines with an IC50 of ~9 J/cm^2 and ~8 J/cm^2, respectively, corresponding to ~12s and ~13.5s exposure duration. In these two cell lines, a dose >20 J/cm^2 led to about 100% cell death. These results were in accordance with previous published studies which showed an antitumor activity of NTP on various cell lines including melanoma, colorectal and hepatocellular carcinoma.[13-19] In our conditions, plasma is generated in ambient air and main active species in the gas are reactive species (RS) such as $OH^{\bullet}$, H_2O_2, N_2*, NO and $O_2^{\bullet -}$. To identify components involved in the *in*

that RS were the main agent involved in this effect. Using H_2O_2 standard concentrations and an oxidant probe dye, an equivalent maximum concentration of 600 μM H_2O_2 after 10 J/cm^2 of NTP was observed. This dye is not specific for H_2O_2 only and DL_{50} of U87MG after H_2O_2 determined by BLI and MTT was 350 μM (data not shown) suggesting that equivalent concentration of H_2O_2 was overestimated and other RS are present in the medium.

After NTP treatment, a cell cycle arrest in S and G2/M phase was observed, confirmed with BrdU incorporation which showed a very low proliferation rate. These data are consistent with those of Yan et al. reporting an *in vitro* cell cycle arrest associated to a modification of cyclin levels with a plasma jet treatment.16 This cell cycle arrest was similar to the multiphase cell cycle arrest observed after ROS exposure with high doses of H_2O_2.29, 30 Dose dependent exposure of ROS leads to cell death,20-22 as observed with NTP. Our data are in strong correlation with those from others studies which reported the effects of NTP on various tumorigenic and non-tumorigenic mammalian cell lines,13-19 thus suggesting a common mechanism of action of NTP, whatever cell type considered.

Radiation therapy, a major antitumor modality that also implies ROS, is able to induce lethal DNA damages which activate cell cycle checkpoints and initiate signaling cascades leading to cell death by generating ROS in cell's DNA vicinity. With NTP, we observed a similar result with the formation of DNA damages in treated cells, leading to cell cycle arrest and finally to cell death with both early and late apoptosis. DNA damages are observed as soon as 1 hr after the treatment, whereas a minimal 3 hr delay is required for phosphorylation of γH2AX histone triggered by apoptosis associated DNA fragmentation.31 This suggests that the signal detected was a direct consequence of the treatment and did not correspond to strand breaks associated with apoptosis induction and subsequent DNA fragmentation. Phosphorylation of γH2AX on Ser139 after DNA damage can be mediated by ATM, ATR and DNA-PK. In a recent work on MCF10A cell line, an induction of γH2AX-phosphorylation was observed after plasma treatment and the authors showed that ATM is not the primary mediator of H2AX phosphorylation on Ser139 as observed after ionizing radiation.19 After NTP treatment, phosphorylation of H2AX occurs primarily through ATR and authors suggest that this activation is the consequences of stalled replication forks formation after NTP. Interaction of plasma with DNA needs further investigation to understand which kind of DNA damage was preferentially induced after treatment.

Given these encouraging results *in vitro*, we further investigated the potential antitumor properties of NTP treatment in human malignant glioma xenografted onto nude mice. In the present study, as compared to nontreated mice, plasma exposure induced a significant inhibition of tumor growth (~40%) at the end of the treatment. This effect is confirmed by BLI, a

xenografts.10 Given the high chemo and radioresistance of the model used here, a significant antitumor effect on such an aggressive tumor model suggests a high efficacy of our approach and evidences the interest of this strategy for cancer therapy. Higher treatment doses should be of valuable interest to enhance this effect more especially that a recent *in vitro* study has also shown an important discrepancy of cell sensitivity between tumor and non-tumor cells.32

The *in vivo* tumor volume and proliferation stabilization obtained could be linked to changes in cell cycle distribution with a decrease in G0/G1 phase and an increase in cells in S phase. Accumulation of tumor cells in S phase caused by plasma may be mediated by DNA strand break formation, even if this point remains to be proven *in vivo*. Moreover, as histologically evidenced, apoptosis induction occurs in the whole tumor. Even if there is no direct evidence that plasma penetrate skin, these data suggest that plasma components act either by penetrating in the tissue either by inducing ROS releases in the tumor. We can also hypothesize that, as described after ionizing radiation treatment, a cell death induced by bystander effect could explain the effect of plasma inside the tumor.33 Even if free radicals only penetrate to a reduced extent into the tissues, this property is of particular interest in the perspective of a direct *in situ* application of NTP for antitumor treatment, avoiding severe systemic side effects. The other components of plasma, such as UV or heat generation, might also play a role in plasma antitumor effect, even if the available data seem only reflect a minor contribution in this effect. Indeed UV penetration in the skin is limited to a few μm and our treatment conditions only generate a temperature increase of about to 3–4°C during a few minutes.26 However, the combination of effects of the different plasma components might result in a synergistic global effect. Indeed, mechanisms of interaction between plasma and cells and plasma skin penetration remain to be further documented since all plasma components could induce membrane damages, changes in intracellular signaling pathways and exhibit cytotoxic properties.

Taken together, our results suggest that NTP could be a new strategy against cancer cells, more especially when used in combination with new generation antitumor drugs. Indeed, recently, Kim et al have demonstrated that association of NTP to EGF-R targeted therapy resulted in a synergistic effect.15 The *in vivo* good tolerability and the effectiveness of NTP towards tumor cells together with the ability to deliver NTP *via* a small capillary open new interesting perspectives for loco-regional or *in situ* applications. Lung and colorectal tumors or dysplasia using plasma endoscopic applications are currently our first therapeutic targets.

Acknowledgements

The authors are grateful to the Region Centre (APR “PlasMed”), Germitec, Conseil Regional du Centre, CNRS and CG45.

References

Citing Literature